Experimental study of uranium carbide pyrophoricity

Clément Berthinier, S. Coullomb, Cyril Rado, Elisabeth Blanquet, Raphaël Boichot, Christian Chatillon

Experimental study of uranium carbide pyrophoricity

C. Berthinier [a], S. Coullomb [a], C. Rado [a,*], E. Blanquet [b], R. Boichot [b], C. Chatillon [b]

[a] CEA, DEN, DTEC, SDTC, LEME, F-30207 Bagnols-sur-Cèze, France

[b] SIMaP, Sciences et Ingénierie des Matériaux et Procédés, (CNRS UMR – 5266 Grenoble-INP/UJF), Phelma, 1130 rue de la Piscine, BP 75, 38402 St Martin-d'Hères, France

Mixed plutonium and uranium monocarbide (UPuC) is considered as a possible fuel material for future nuclear gas fast reactors. Its safe handling is currently a major concern, because inflammation of this material under the shape of fine powders is easy and highly exothermic (pyrophoricity) even under ambient temperature and partial pressure of oxygen inferior to 0.2 bar. CEA Marcoule is implied in both experimental and numerical studies on the UC powder oxidation exothermic reaction. Experimental tests consist in determining the influence of various parameters (gas composition, heating ramp, specific surface of powders) on the sample inflammation temperature. Two kinds of analytical apparatus are used: The differential thermal analysis (DTA) and the differential scanning calorimetry (DSC) coupled to the thermo gravimetric analysis (TGA). These apparatus are also linked to a gas mass spectrometer to follow the composition of combustion chamber gases. Results obtained with small quantities revealed that UC powder is highly reactive in air in the temperature range of 150–250 °C and showed a strong dependence between powder height in crucibles and inflammation temperature.

1. Introduction

Mixed uranium and plutonium carbide (U,Pu)C, constituted by about 80% of uranium monocarbide (UC), is considered as a possible fuel material for future gas fast reactors or sodium fast reactor. As UC or (U,Pu)C undergoes a strong exothermic reaction with air (fine powders of UC are pyrophoric), it is necessary to understand this high reactivity in order to determine safe handling conditions for the production and reprocessing of carbide fuels [1]. In order to favor easier experimental conditions, studies on pyrophoricity [2,3] at CEA Marcoule are first performed on low radioactivity uranium monocarbide UC. These experiments are the continuity of several works on the same subject [4–6].

2. Experimental procedure

Samples of uranium monocarbide with an approximate weight of 1 g were prepared by arc-melting of solid uranium metal and carbon graphite under argon. UC ingots were then ground for 5 h in dodecane to prevent oxidation.

The laser particle size measurements data are listed in Table 1.

The powder was then stored in dodecane. In order to remove dodecane, the UC and dodecane mixture were loaded in a crucible using a micro spoon spatula and either dried for 24 h at 50 °C in a 10^{-2} mbar dynamic vacuum or dried for 24 h at 50 °C in air.

After drying, powder forms a crust which disaggregates when scraped with a spatula. Characterization by X-ray diffraction of the dried powder in air showed no oxides i.e. no oxide layer was observed at the micrometric scale, which does not discard any native thin oxide layer. However, no differences on pyrophoricity were observed between UC dried in dynamic vacuum or dried in air. Finally before the oxidation tests, the UC powders were simply dried for 24 h at 50 °C in air. The specific surface area of the powder, dried and disaggregated, measured by a Micromeritics ASAP, 2010 is 2 m^2/g.

Oxidation tests were first performed in a Setaram DSC 131. The device operates with flowing air or various other gases. Differential scanning calorimetry (DSC) is a measure of the temperature and temperature derivative vs. time between the sample and a reference. Temperatures are imposed by programmed ramps under controlled atmospheric pressure flow. The sample (UC and dodecane) is loaded in a 6.2 mm internal diameter and 2.8 mm height cylindrical aluminum crucible and dried in air. The dried mass of UC powder used for the DSC tests was between 19 mg and 100 mg.

Oxidation experiments were also performed in an alumina internal structures Setaram TGA92 DTA/TGA thermobalance. Differential thermal analysis (DTA) consists in measuring the temperature difference between the sample and a reference versus time during heating or cooling. The sample (UC and dodecane) is loaded in a 4 mm internal diameter and 8 mm height cylindrical alumina crucible and dried in air. The dried mass of UC used for the DTA tests was between 17 mg and 150 mg. The sample was then placed in the thermobalance.

* Corresponding author.
E-mail address: cyril.rado@cea.fr (C. Rado).

Table 1
Particle size distribution of UC powder.

Milling time	D_{10} (μm)	D_{50} (μm)	D_{90} (μm)
5 h	1.3	2.7	5.0

Using TGA simultaneously, the sample weight gain was also monitored. A Pfeiffer Omnistar™ mass spectrometer is also coupled to the thermobalance in order to follow the concentration of gases in time.

Tests in DSC and ATD were carried out under a controlled dry air flow rate of 3 l/h. After a holding time of 1800 s at room temperature to stabilize both air flow and temperature, the sample is then submitted to a 5 °C min^{-1} temperature ramp up to 500 °C. The ignition point was identified as the point of intersection of the tangents to the curves before and after excess heat exchange.

At the end of the test, the oxidized powder was allowed to cool down to room temperature (switching to pure Argon flow at the same time). The sample is then collected in silicone grease mixed with Ta powder for X-ray diffraction analysis.

3. Results

Tests were performed in DSC using the experimental procedure defined just before. Ignition temperatures were measured between 166 °C and 267 °C. Fig. 1 presents a typical curve, with mainly an exothermal differential peak around 200 °C, and a 40° increase of the temperature measured under the crucible. After the peak, the ignition pertains with a small exothermal effect (≈10 mW).

In order to identify the phases formed by reaction of UC with air by XRD analysis, tests were stopped at different temperatures and air was replaced by a pure argon flow before cooling down to room temperature at 20 °C min^{-1}. Results of XRD analysis after each shutdown are listed in Table 2 and compared with DSC analysis in Fig. 2.

When stopped at 170 °C during the first slow thermal effect before ignition, there is no detectable new formed phase according to XRD. By stopping the heating at 200 °C (the early beginning of the ignition), we observed UC and already some oxides. After the ignition peak, the product is mainly U_3O_8 but intermediate compounds are still observed with maybe some residual UC core. The final transformation of UC into the stable oxide at air U_3O_8 occurs in the range of 390–430 °C.

Experiments were performed using the same experimental procedure in DTA/TGA. We have to quote that for UC masses typically smaller than 30 mg the ignition was not observed. For larger masses two main exothermic peaks were observed on the DTA curve as presented in Fig. 3 (samples between 30 and 60 mg).

Table 2
XRD characterization of the phases at different shut down temperatures in the DSC tests.

Shut down temperature	Ignition	XRD phases identification
170 °C	No	UC
200 °C	195 °C	$UC + U_3O_8 + UO_{2+x} + U_3O_7$
250 °C	187 °C	$U_3O_8 + UO_{2+x} + U_3O_7$ + UC ?
390 °C	203 °C	$U_3O_8 + UO_{2+x} + U_3O_7$
430 °C	170 °C	U_3O_8
500 °C	223 °C	U_3O_8

A strong exothermic reaction characterized by a sharp heat flow peak occurred around 200 °C and corresponds to ignition, with a temperature increase above 100 °C/min. Ignition temperatures were measured between 198 °C and 270 °C (average ignition temperature = 233 °C). A second exothermic reaction characterized by a smaller heat flow peak occurred around 400 °C with mass loss. Between these two heat flow peaks, reaction goes on with a positive heat flow peak and a mass gain.

The mass is continuously increasing during inflammation (Fig. 4). At about 5600 s, the sample mass reaches a stable value, overshooting the 12.27% mass gain that should be obtained if all the UC powder is converted into U_3O_8. Then from 6200 s, mass decreases to stabilize at the theoretical 12.27% mass gain.

Three sharp CO_2 peaks are measured by the mass spectrometer during UC reaction with oxygen (Fig. 5). The first small peak logically corresponds to UC ignition at 4500 s. The second and most important peak is released during the sample mass overshoot. Finally a third CO_2 release corresponds in time to the beginning of the mass loss. Oxygen exhibits the same – but inverted – trend (Fig. 5). The O_2 peak intensities are not proportional to CO_2 peak intensities: the most important O_2 depletion corresponds to ignition time. CO is briefly formed in small quantities at the beginning of the first CO_2 release and O_2 depletion.

Two experiments performed with increasing masses of sample (77 and 147 mg) showed a large exothermal peak at about 200 °C followed by a second one at about 250 °C with powder projections outside the crucible.

In order to identify the phases formed by reaction of UC with air by XRD analysis, experiments were stopped at different temperatures. Pure argon flow was used to cool down the sample to room temperature at 20 °C min^{-1}. Phases measured by XRD analysis after each shutdown are listed in Table 3 and compared with DTA analysis in Fig. 6.

When comparing Tables 2 and 3, it is clear that conversion of UC into U_3O_8 was observed to be faster in our DSC than in our DTA

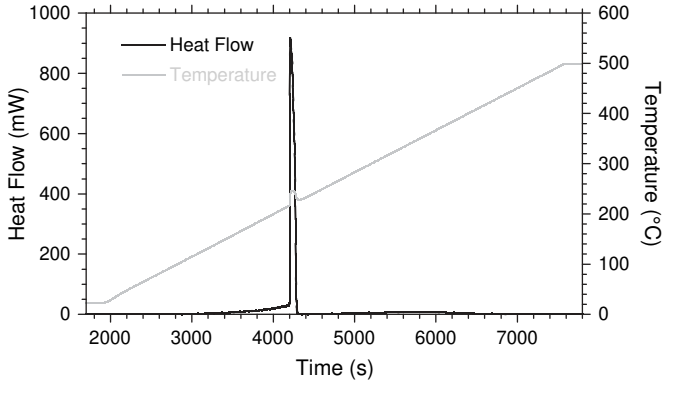

Fig. 1. Temperature as measured under the crucible (grey curve) and thermal energy exhaust (black curve) during a DSC experiment.

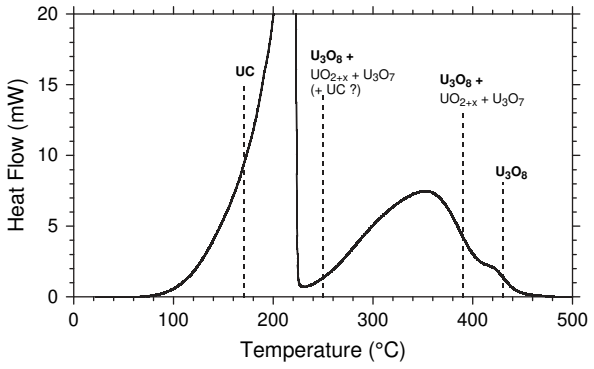

Fig. 2. XRD analysis results compared with DSC analysis.

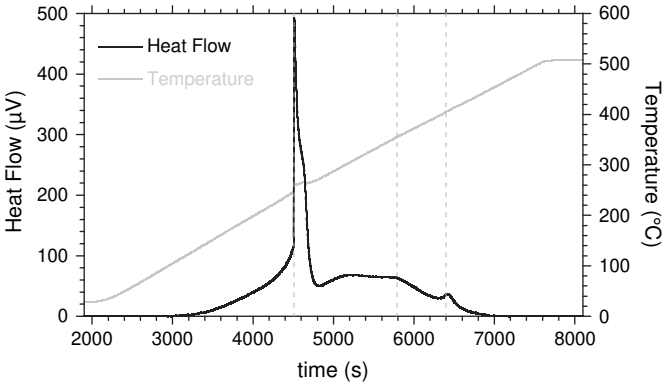

Fig. 3. Typical differential thermal analysis obtained at 5 °C min^{-1} up to 500 °C under dry air (3 l/h).

experiments. In DSC, UC is mainly converted into U_3O_8 just after ignition, even though only the intermediate oxide UO_2 is formed just after ignition in DTA apparatus.

In order to understand why oxidation reaction seems faster in DSC, we first test the inlet gas flow rate influence in DTA configuration. It appears that this parameter has no influence on the velocity of chemical reaction (Fig. 7). This means physically that chemical reaction is not affected by gaseous reactant velocity field around the DTA crucible.

Tests were carried under pure oxygen in DTA configuration. In this case where oxygen transport is not limited by nitrogen, the chemical reaction is relatively similar to the DSC configuration (Fig. 8): the inflammation is sharp and releases mainly the totality of heat flow. Differences in behavior with these two configurations should be due to geometrical artifact. The crucible shape in DTA configuration smothers the chemical reaction. This point is discussed further.

We also observe a slight scattering of ignition temperature with the UC powder mass used in crucibles. DSC and DTA tests were carried out to estimate the influence of the powder mass, so the powder height, in crucibles, on the ignition temperature. For these tests, the powder is first dried in air and then disaggregated with a spatula before being placed in DSC or DTA crucible. This avoids powder to form solid cake with unpredictable shape after drying. Samples are then dried once again in a 3 l/h air flow rate during 1800 s and heated by a 5 °C min^{-1} ramp toward 500 °C (classical procedure).

Inflammation temperature plotted against powder height in crucibles is represented in Fig. 9.

The influence of this parameter is discussed in discussion section.

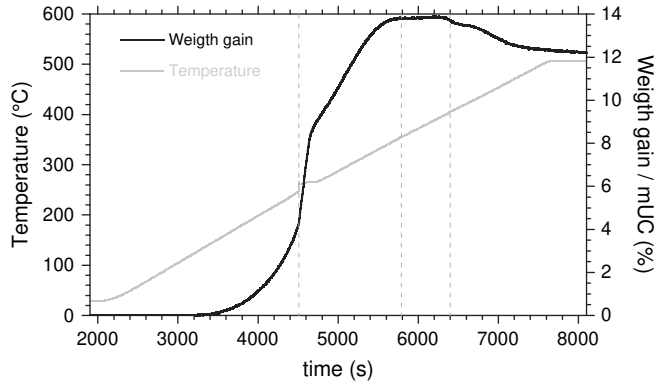

Fig. 4. Thermogravimetric Analysis obtained at 5 °C min^{-1} up to 500 °C under dry air (3 l/h).

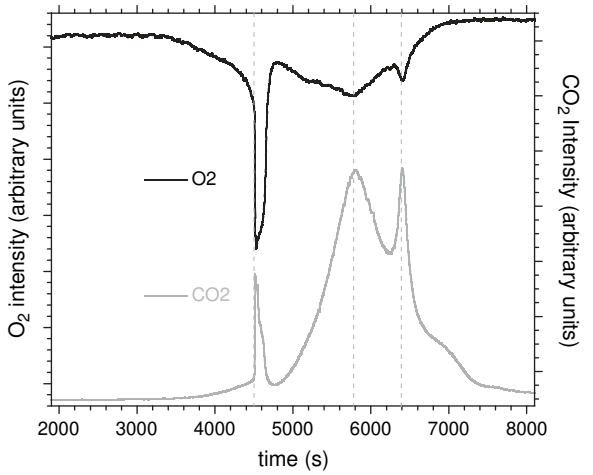

Fig. 5. Mass Spectroscopy Analysis of O_2 and CO_2 obtained at 5 °C min^{-1} up to 500 °C under dry air (3 l/h).

4. Discussion

4.1. Phase diagrams, reaction path and formed species

The context of the ignition reactions has been first developed on a thermodynamic basis [2]. The possible products that can be formed in the ignition reaction are given by the trajectory followed in the ternary U–C–O phase diagram from UC to O_2. Fig. 10 shows a calculated isothermal section at 500 K close to the ignition temperature range.

From this phase diagram – the shape of which is the same at least up to 1600 K – the attended ignition products may be the solid solution UCO, the oxide compound UO_2 and higher O content oxides, as well as the carbide U_2C_3 and carbon. Note that due to sluggish formation of this carbide, the UC_2 could be formed instead. At the same time CO (g) and CO_2 (g) – not represented in this section – can be produced at a pressure which is depending on the different triphasic domains as already discussed [2]. Among these different products, the formation of UO_2 is by far the main heat source and it has to be produced at first. Further oxidation into U_3O_8 – which is the stable one at atmospheric pressure up to 870 K – will provide a supplementary heat production. At the same time, CO and CO_2 gases are produced that might prevent the oxygen flow to reach the surface of the solids. As evaluated in the preceding work [2], we found that the calculated thermodynamic $CO + CO_2$ pressure increases toward 1 bar when solid C is in equilibrium with stoichiometric or slightly hyperstoichiometric UO_2.

For DSC experiments, inflammation mainly leads to U_3O_8 formation and to a small amount of UO_{2+x} and U_3O_7 for the test stopped at 250 °C. Typically in DSC, the fast and complete reaction does not allow to identify intermediate oxides or steps during UC oxidation.

On the other hand, DTA experiments highlight that just after inflammation, different oxides still remain in the crucibles with fresh UC: UO_{2+x} and U_3O_7. At a more advanced state (380 °C) UC becomes

Table 3
XRD characterization of the phases at different shut down temperatures in the DTA tests.

Shut down temperature	Ignition	XRD phases identification
200 °C	no	UC
300 °C	241 °C	$UC + UO_{2+x} + U_3O_7$
380 °C	237 °C	$UO_{2+x} + U_3O_7 + U_3O_8$
420 °C	240 °C	U_3O_8
500 °C	252 °C	U_3O_8

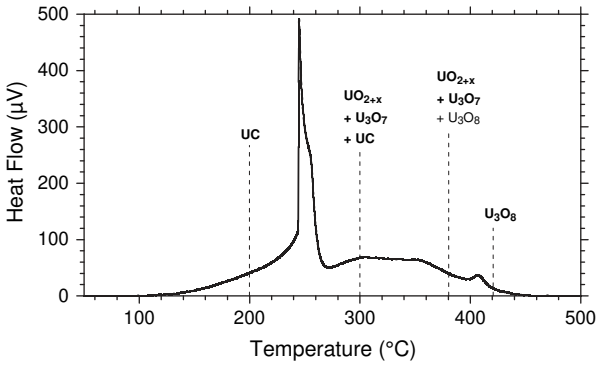

Fig. 6. Typical differential thermal analysis graph altogether with identified phases at different temperatures.

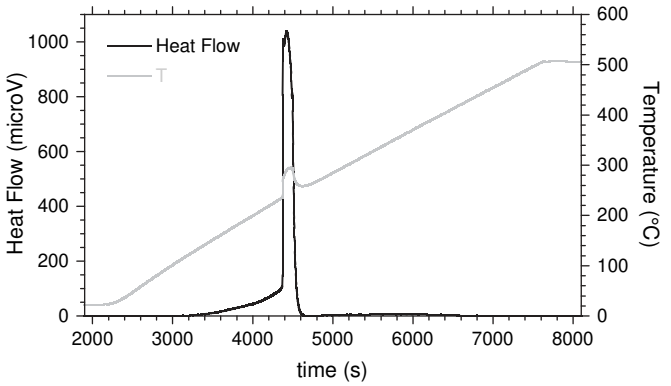

Fig. 8. DTA experiment under pure oxygen (3 l/h).

not detectable in DRX. The remaining powder is mainly UO_{2+x} and U_3O_7 with a small quantity of U_3O_8.

For both DSC and DTA, the complete oxidation toward U_3O_8 is reached at 400 °C.

The overall conversion of UC into U_3O_8 occurs at about 400 °C. According to Dehaudt [7] compilation, the UO_2 oxidation into U_3O_8 goes through the intermediate U_3O_7 oxide very often. For temperatures lower than 250 °C, the U_3O_8 nucleation becomes very slow and the whole mass of UO_2 can be transformed into U_3O_7 before any U_3O_8 appearance. For higher temperatures – typically 250–300 °C – the U_3O_7 oxide is never observed detrimental to the rapid appearance of U_3O_8. Table 4 presents the time needed for a total transformation of UO_2 into U_3O_8 according to Dehaudt [7].

In our experiments with ignition, the observed intermediate phases are UO_2 and U_3O_7 whatever the technique. In the anisothermal experiments, the end of the transformation of UO_2 or U_3O_7 into U_3O_8 is observed between 380 and 420 °C in DTA, and between 390 and 430 °C in DSC. This 40 °C range obtained with a 5 °C ramp corresponds to a complete transformation within 8 min. This duration agrees with the Dehaudt's [7] work for isothermal experiments.

In DTA experiment, the sample mass gain overshoots the predicted value and reaches 14% more than the initial UC mass. Indeed, the complete oxidation of UC to U_3O_8 with C elimination under gaseous CO_2 form would produce a 12.27% mass gain. This latter mass gain is effectively obtained at 500 °C. This means clearly that stable solid carbon is formed and trapped inside the sample during oxidation. DRX analysis does not highlight any UC_2 or U_2C_3 phase. Carbon certainly remains under the form of fine amorphous precipitates as observed in the case of UC_2 oxidation by Nawada et al. [8,9]. This non-equilibrium state cannot be predicted by Fig. 10 phase diagram.

Gas analysis (Fig. 5) during inflammation shows a brief CO_2 peak and an important O_2 consumption. This could be the consequence of a massive UO_2 formation coupled to solid C trapped locally or attacked by O_2 due to localized overheating.

After inflammation, CO_2 release becomes very intense at 360 °C. At this step, UC continues to react to form UO_2 near the center of the sample but the oxygen pressure should increase at the periphery of the sample, allowing a solid C partial combustion. The heat of combustion of UC to UO_2 could also locally promote C combustion by overheating the sample. UO_2 should react to form U_3O_8 where partial pressures of O_2 are high.

At 410 °C, another brief but intense CO_2 peak is observed, the mass suddenly decrease to the theoretical value. All UC is ever transformed into UO_2, the partial pressure of O_2 is high and the temperature is high enough to complete C combustion in the entire sample. This is also promoted by the fact that UO_2 is transformed into U_3O_8 which is highly fragmented, facilitating O_2 transport into the sample.

4.2. Reaction kinetic: DTA and DSC difference

The geometry of the two crucibles – DTA and DSC – is presented in Fig. 11. In the case of DSC crucibles, the shape favours the oxygen introduction compared to DTA crucibles. In the last case the oxygen admission could be lower. Indeed, the products CO and CO_2 formed by the ignition flows in an opposite direction than oxygen, forming a resistance to mass transport in the DTA alumina tube. The oxidation rate should consequently decrease.

The input flows in the two apparatus are clearly different as shown in Fig. 12. The DSC geometry seems more efficient in CO_2 elimination by diffusion (larger surface exchange, smaller height of the tube wall).

In DTA configuration, doubling the gas flow rate from 3 to 6 l/h did not accelerate the oxidation reaction (Fig. 7). Beside this, DTA experiment conducted in pure oxygen gives a fast reaction as in DSC

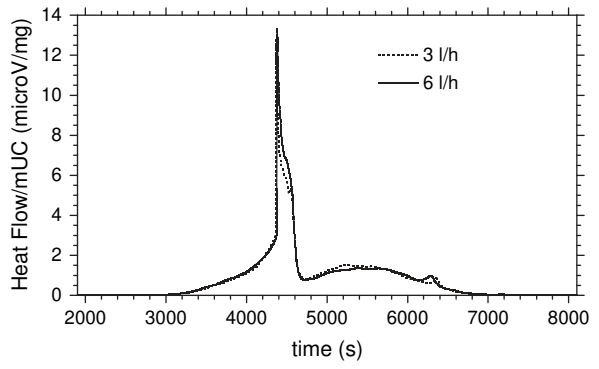

Fig. 7. DTA analysis under 3 l/h and 6 l/h dry air flow rate.

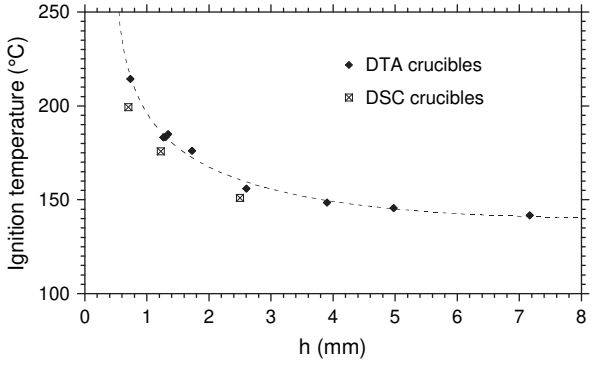

Fig. 9. Ignition temperature versus powder bed height in DTA crucibles (♦) and DSC crucibles (⊠).

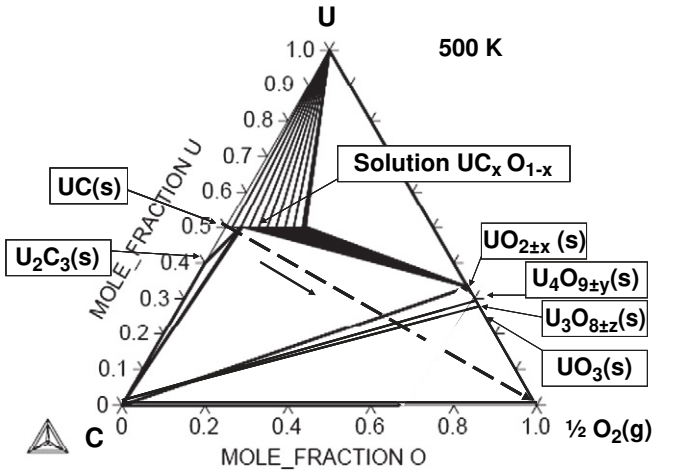

Fig. 10. Calculated ternary U–C–O phase diagram at 500 K. The arrow shows the mean composition trajectory for the ignition products, starting from UC(s) and going towards O_2(g).

configuration (Fig. 8). It seems that the DTA crucible acts as a mass transport resistance due to its shape.

4.3. Ignition temperature scattering

We found no influence of gas composition on ignition temperature (100% O_2 or dried air). This result is consistent with the study of Dell and Wheeler [4] and Sowden et al. [6]. According to Sowden et al. [6] decreasing the oxygen partial pressure does not modify the ignition temperature but of course decreases the reaction rate. This could be understood by the fact that ignition temperature is due to activation energy (limitation by reaction), not depending on concentrations, contrary to the reaction kinetic (limitation by transfer).

Different experiments performed with similar UC masses, gas flows and temperature ramps in the two apparatuses show the same behavior up to ignition: heat production starts at 100 °C. Further, a large scatter is observed for the ignition temperature whatever the apparatus.

Besides, the {dodecane + UC} mixture is viscous and its loading in the crucibles may be done in a non reproducible way. After drying, for the same weight loaded, different shapes are observed as illustrated in Fig. 13. So, the observed scattering of the ignition temperature in DTA and DSC should be related to the shape and repartition of the powder sample.

Experimental tests (done with a well controlled disaggregated dried powder) exhibit a comparable influence of powder thickness on ignition temperature, both in DTA and DSC configuration (Fig. 9). In DTA configuration, we observe no ignition for very thin layer of UC powder (for example a 19.6 mg powder mass and 0.48 mm thickness layer). The ignition temperature globally follows a decreasing law toward stabilization at around 6 mm of powder thickness. This phenomenon confirms the fact that the powder layer undergoes different reaction paths according to the oxygen availability: it is possible here that for the first reaction step ($UC \rightarrow UO_2 + C$) the active powder layer is limited to around 4 mm. Under this thickness no reaction can occur because O_2 is trapped by the upper UC layer.

The thicker the active layer (layer that have access to O_2), the lower the ignition temperature due to a mass effect. The radiation surface (that evacuates reaction heating) remains the same even though the active mass increases with powder thickness.

In DSC and DTA configuration, when the powder is dried into the crucibles and not scraped, we pour the UC + dodecane coming from grounding under the form of a viscous paste.

This leads to a UC base that forms a little mound in DSC configuration (Fig. 13a). The ignition temperature is lower than with a constant thickness layer having the same UC quantity. Indeed, locally, the UC thickness can be high (Fig. 14). According to the viscosity of the mixture, UC + dodecane can also adhere to the wall and forms a meniscus. In this case the ignition temperature is higher than expected.

In ATD configuration, the crucible is narrower than in DSC, and the mixture tends to systematically form a meniscus (Fig. 13c). Logically the ignition temperature is higher than expected (Fig. 14).

Table 4
Duration needed for a total transformation of UO_2 into U_3O_8 as a function of temperature according to Dehaudt [7].

T (°C)	Duration (min)
350	71
375	24
400	8.7
425	3.4
450	1.4

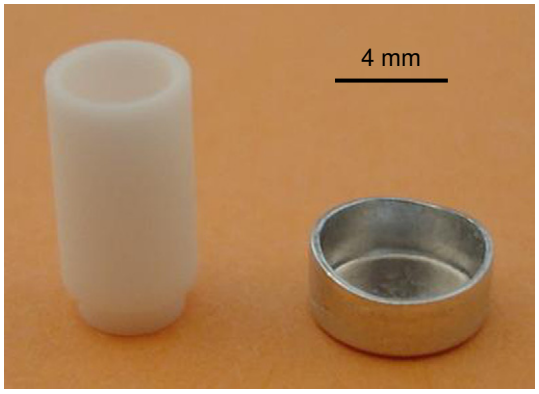

Fig. 11. DTA (left) and DSC (right) crucibles.

4.4. Numerical simulation

Chemical reaction of UC with oxygen products several oxides – UO_{2+x}, U_3O_7 and U_3O_8 – and gaseous species — CO and CO_2. The global reaction can be written as follows:

$$UC + 7/3\ O_2 \rightarrow 1/3\ U_3O_8 + CO_2. \quad (1)$$

The phenomenon is in real configuration more complex. UC react first with O_2 to form UO_{2+x}, U_3O_7 and U_3O_8, depending on the local availability of oxygen into the powder layer. Then carbon is released in oxides and trapped or directly attacked according to local overheating and also oxygen availability. Each reaction release heating and/or gaseous heated species. The sample itself evacuates heat by conduction and radiation with the crucible and environment. Finally the reactant intake is influenced by the shape and environment of the crucible. If the local balance between reaction heat and

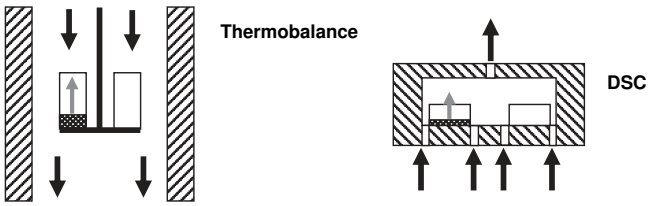

Fig. 12. Air flow diagram (black arrows) and gas products flows (grey arrows) sketched for the two apparatuses.

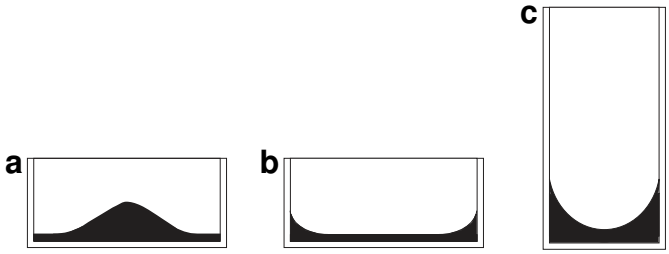

Fig. 13. Schematics of typical powder sample shapes observed after the drying step. Left (a and b): DSC crucibles. Right (c): DTA crucibles.

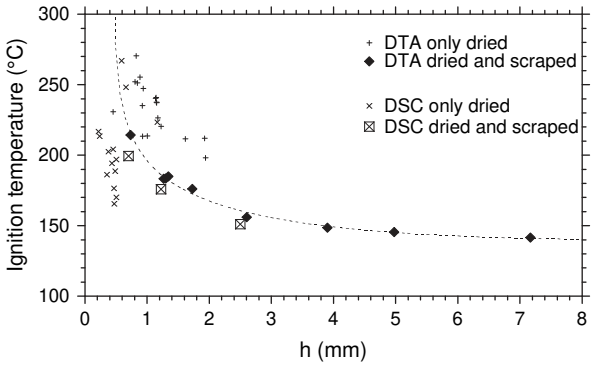

Fig. 14. Ignition temperature vs powder bed height in DTA crucibles and DSC crucibles. DTA ♦ and DSC ⊠: UC powder dried and scraped (the powder bed height is well controlled). DTA + and DSC ×: UC powder only dried in the crucibles (the powder height is calculated from UC mass and do not take into account the powder sample shape).

evacuated heat is positive, the reaction is self sustained, and can propagate to all the powder while the oxygen intake is sufficient.

To model an accidental scenario, DSC and DTA experiments are not sufficient, because the powder configuration seems to play a crucial role. Understanding the behavior of U–C–O ternary diagram is necessary, but it is also imperative to model reactants and heat transport around the powder and inside it.

Numerical CFD simulations are currently constructed to take into account all these parameters. The first results we obtained give accurate prediction of UC powder ignition point and mass evolution. DSC and DTA experiments are now used to calibrate this simulation. In a near future this simulation will serve as a safety tool once it will be completely checked.

5. Conclusions

In a first attempt and to allow easier experimental conditions, pyrophoricity tests were undertaken on uranium monocarbide (UC) with the aim to determine safe handling conditions for the production and reprocessing of mixed uranium and plutonium carbide. The behavior of UC powders in air has been studied in different apparatus that presented different geometrical configurations. Using small and comparable quantities in DSC and in DTA/ATG experiments showed that – (i) ignition temperatures as determined by the first heat exhaust peak are slightly different but remain quite scattered – (ii) ignition peak may be single or double (sometimes triple) depending on the container geometry – (iii) products compositions revealed differences in the phases proportions but not in the products nature. This last observation shows that the ignition reactions are occurring as a complex process in which the chemical species transport can spread the ignition in time scale.

Auto-ignition temperatures vary from 166 to 267 °C in DSC experiments in air; meanwhile this range becomes 198 to 270 °C in DTA. For DSC experiments the ignition is quite spontaneous and complete at 250 °C as revealed by the main U_3O_8 oxide product. In DTA experiments, the ignition is still not complete at 300 °C with a $\{UC + UO_{2+x} + U_3O_7\}$ mixture with quite equal compound contents.

Differences in the behavior of the powders were mainly attributed to the geometry of the crucibles and the powder beds height, and consequently to a lower extent to the convective gas flow fields around the crucibles. For DSC experiments, a large diameter associated to a small height favours the gas exchange and the ignition reaction occurs in one important step, meanwhile in DTA experiments an exhaust of gas products (CO and CO_2) through a small section and quite deep crucible can choke the oxygen input flow. So, for this last case, a succession of peaks can be observed.

Dedicated experiments showed a strong dependence between powder height in crucibles and inflammation temperature. This temperature decreases with the increase of powder height toward a stabilization around 4 mm thickness.

All these observed mechanisms – in relation with the powder quantity and the container shape – will allow the modelling of heat exchange and mass transport on clear basis.

Acknowledgment

The authors wish to thank the DTEC/SGCS/LMAC for SEM and XRD analysis.

References

[1] P. Martin, N. Chauvin, J.C. Garnier, M. Masson, P. Brossard, P. Anzieu, Gas cooled fast reactor system: major objectives and options for reactor, fuel and fuel cycle, Proceedings of GLOBAL 2005, 2005, Tsukuba, Japan.
[2] F. Le Guyadec, C. Rado, S. Joffre, S. Coullomb, C. Chatillon, E. Blanquet, Thermodynamic and experimental study of UC powders ignition, Journal of Nuclear Materials 393 (2009) 333–342.
[3] F. Le Guyadec, S. Joffre, C. Chatillon, E. Blanquet, Oxydation et évaluation de la température d'inflammation de poudres d'UC et d'UN, Proceedings of Matériaux 2006, 13–17 November, 2006, Dijon, France.
[4] R.M. Dell, V.J. Wheeler, The ignition of uranium mononitride and uranium monocarbide in oxygen, Journal of Nuclear Materials 21 (1967) 328–336.
[5] S.K. Mukerjee, G.A. Rama Rao, J.V. Dehadraya, V.N. Vaidya, V. Venugopal, The oxidation of uranium monocarbide microspheres, Journal of Nuclear Materials 210 (1994) 97–106.
[6] R.G. Sowden, N. Hodge, M.J. Morton-Smith, D.B. White, The behaviour of carbides in hydrogen and oxygen, Proceedings of a symposium held at Harwell, Nov 1963, Carbides in Nuclear Energy, vol. 1, 1964, pp. 297–314.
[7] P. Dehaudt, Oxidation of nuclear fuel below 400 °C. Consequence on long-term dry storage, 2000 CEA-R-5924.
[8] H.P. Nawada, P. Srimana Murti, G. Seenivasan, S. Anthenysamy, C.K Mathews, Thermogravimetric study of the oxidation behaviour of uranium dicarbide, Journal of Thermal Analysis 35 (1989) 1145–1155.
[9] H.P. Nawada, P. Srimana Murti, G. Seenivasan, S. Anthenysamy, A thermoanalytical study of the ignition behaviour of uranium dicarbide, Thermochimica Acta 144 (1989) 357–361.